

Available online at www.sciencedirect.com

SciVerse ScienceDirect

Procedia Environmental Sciences 18 (2013) 472 – 477

Procedia

Environmental Sciences

2013 International Symposium on Environmental Science and Technology (2013 ISEST)

Sorption of perfluorooctane sulfonate (PFOS) on electrospun fiber membranes

Jiangjie Xu, Junfeng Niu*, Siyuan Zhang

State Key Laboratory of Water Environment Simulation, School of Environment, Beijing Normal University, Beijing 100875, China

Abstract

Poly(d,l-lactide-co-glycolide) (PLGA) and polyvinyl alcohol (PVA) were used to prepare the electrospun fibers membranes (EFMs) by electrospinning, respectively. These EFMs were used to adsorb perfluorooctane sulfonate (PFOS) from aqueous solution. The sorption kinetics and isotherms of PFOS on EFMs were investigated. The pseudo-first-order model (PFOM) can well describe the sorption kinetics of PFOS on these two types of EFMs. The experimental results show that the sorption capacities of PFOS on PLGA and PVA EFMs are 77.29 and 337.77 $\mu\text{g}\cdot\text{g}^{-1}$, respectively. The main sorption mechanisms of PFOS on PLGA EFMs are pore-filling. Moreover, hydrogen bonding interactions exist in the sorption processes of PFOS on PVA EFMs.

© 2013 The Authors. Published by Elsevier B.V. Open access under [CC BY-NC-ND license](#).
Selection and peer-review under responsibility of Beijing Institute of Technology.

Keywords: Perfluorooctane sulfonate; electrospun fibers membranes; sorption kinetics; sorption isotherms

1. Introduction

Perfluorooctane sulfonate (PFOS), as a commonly used anionic surfactant, has been widely used in industry since the early 1970s [1]. During 1970 – 2002, an amount of 45250 t PFOS had been released into air and surface water [2]. It has been detected in human tissue at a relative high level [1]. Unfortunately, PFOS was listed as a persistent organic pollutant in Stockholm Convention in 2009. It can disturb lipid metabolism and lead to the accumulation of excessive fatty acids and triglycerides in hepatocytes [3].

Many methods including adsorption[4], plant uptake[5], oxidation[6] and sonochemical degradation[7] are developed to remove PFOS from water. Most chemical reactions are difficult to occur at mild condition due to the persistent nature of PFOS. Therefore, sorption treatment is considered as a satisfying choice to remove PFOS from water since it is simple and cost-effective. Some types of sorbents have

* Corresponding author. Tel.: +86-10-5880 7612; fax: +86-10-5880 7612.
E-mail address: junfengn@bnu.edu.cn.

been reported to be effective for PFOS removal, such as carbon nanotubes [8], alumina [9], and boehmite [10]. However, these sorbents are difficult to be recycled from water since they generally exist in the form of powders or particles. Therefore, it is of great importance to find out a recyclable, high-efficient sorbent.

Electrospun fibers membranes (EFMs), as a simple and low-cost technique, have many novel characters, such as porous structure, high surface-to-volume ratio and well mechanical properties [11]. These characters make EFMs adsorb more pollutant and easier to be recycled [12, 13]. Recently, EFMs have been used as sorbent for the adsorption of heavy metal ion [14], polycyclic aromatic hydrocarbons (PAHs) [15] and oil [16]. However, few researches about the sorption of PFOS from water using EFMs have been reported.

In this paper, two types of polymers with different structures and properties (PLGA and PVA) were used to prepare the EFMs by electrospinning. The sorption kinetics and isotherms of PFOS on EFMs were investigated.

2. Materials and Methods

2.1. Materials

Poly(D,L-lactide-co-glycolide) (PLGA) (molecular weight = 100 000 g·mol⁻¹) was purchased from Jinan Daigang biomaterials Co., Ltd. (China). Polyvinyl alcohol (PVA) was obtained commercially from Sinopharm Chemical Reagent Co., Ltd. (China). Triblock copolymer PEO-PPO-PEO (F108) was supported by BASF (Germany). Methylene dichloride and methanol (HPLC, 99.9%) were provided by J.T.Baker (USA). All other reagents were of analytical grade, without further purification. All solutions were prepared using high-purity water obtained from a Milli-Q Plus/Millipore purification system.

2.2. Preparation of electrospun fibrous membranes

Electrospinning was carried out on a self-made electrospinning apparatus in our laboratory. The procedures for the PLGA EFMs were as follows: Firstly, 1.8 g PLGA and a certain amount of F108 were dissolved in 15 g methylene dichloride with stirring for 2.0 h at ambient temperature to form a homogeneous solution. Then, the homogeneous solution was loaded into a stainless glass syringe, which was equipped with a clean needle (0.5 mm inner diameter) and connected with a high-voltage power supply (HB-Z503-2AC, China). Electrospinning was operated at a voltage of 10 ± 1 kV, and the homogeneous solution was fed at a rate of 1.5 mL·h⁻¹ by using a syringe pump (RWD Life Science Company Limited, China). A grounded iron plate covered with aluminum foil was placed at a distance of 15 cm from the needle tip as a fiber collector. It usually took 3 - 5 h to obtain integrated and sufficiently thick EFMs. For PVA EFMs, the homogeneous solution was prepared by dissolving 1.2 g PVA and a certain amount of F108 in 18.8 g high-purity water. The remaining processes were the same as preparing PLGA EFMs. All experiments were conducted at room temperature ($25^\circ\text{C} \pm 1^\circ\text{C}$) and a relative humidity of $40\% \pm 2\%$.

2.3. Characterization

The morphology of EFMs was observed with a field emission scanning electron microscope (FESEM S-4800, HITACHI, Japan). The diameter of fiber was calculated from more than 100 counts randomly selected from 10 different SEM images.

2.4. Sorption experiments

All sorption experiments were conducted in 150 ml polypropylene copolymer (PPCO) conical flasks containing three pieces of EFMs (2 cm × 2 cm, total weight 50 ± 2 mg) and 50 mL of PFOS aqueous solution. The conical flasks was shaken at 150 rpm and kept at 25 ± 1 °C. In the experiment, sorption kinetic was conducted with an initial PFOS concentration of 100 µg·L⁻¹. The sorption isotherm experiment was carried out with the initial PCP concentration ranging from 20 µg·L⁻¹ to 1000 µg·L⁻¹. According to the preliminary experiment, adsorption equilibrium was reached when the experiment running 120 min. A volume of 1.5 mL reaction sample was taken from the reaction system at certain time intervals for high-performance liquid chromatography-tandem mass spectrometry (HPLC-MS/MS) analysis. Experimental uncertainties evaluated in samples without EFMs were less than 5% of the initial concentrations. All samples were produced in triplicates including control, and the average value was adopted.

2.5. Sorption kinetics and isotherm models

Two commonly used isotherm models, Langmuir model (LM) and the Freundlich model (FM) were used to fit the isotherm experiment data, and then to compare their goodness of fitting. Moreover, for analyzing the adsorption kinetic data, pseudo-first order model (PFOM) and pseudo-second order model (PSOM) were used. The parameter values of all models were calculated by means of the nonlinear curve fitting analysis. The sorption isotherm and kinetics models are listed in Table 1 .

Table 1. Sorption isotherm and kinetics models.

Category	Name	Abbr.	Equation	Capacity term
Sorption isotherm models	Freundlich model	FM	$q_e = K_f C_e^{1/n}$	$K_f [(\mu\text{g/g})/(\text{mg/L})^{1/n}]$, Freundlich affinity coefficient; 1/n, Freundlich exponential coefficient.($n^{-1} = 1$ means a linear isotherm, no sorbate-sorbate interaction exists)
	Langmuir model	LM	$q_e = Q_0 C_e / (K_1 + C_e)$	$K_1 [\mu\text{g/L}]$, affinity coefficient.
Kinetics models	Pseudo-first order model	PFOM	$q_t = q_e (1 - e^{-k_1 t})$	$k_1 [\text{h}^{-1}]$, rate constant of the pseudo-first order model.
	Pseudo-second order model	PSOM	$q_t = q_e k_2^* t / (1 + k_2^* t)$	$k_2^* = k_2 q_e$, $[\text{h}^{-1}]$, k_2 , the rate constant of the pseudo-second order equation.

q_e , equilibrium sorption amount (µg·g⁻¹);

C_e , equilibrium solution phase concentration (µg·L⁻¹);

Q_0 , sorption capacity (µg·g⁻¹);

q_t , sorption amount at time t (µg·g⁻¹);

3. Results and Discussion

3.1. Morphology of electrospun fibrous membranes

As shown in Fig. 1, the SEM images of EFMs exhibited some different characteristics. PLGA fibers possessed the feature of bead-free and porous. Whereas, PVA fibers contained plenty of beads and no pores were detected. In order to explain the difference of pores, breath figures, which are commonly used to explain the formation of pores on electrospun fibers, are introduced [17]. Breath figures form due to evaporative cooling. As the electrospinning jet is being propelled toward the target, the surface of the jet cools and water from the air condenses on the surface of the fiber. As the fiber dries, the water droplets leave an imprint behind [18]. The solvent of PLGA is methylene dichloride, which is not miscible with water. Therefore, water from the air can leave an imprint behind on the surface of PLGA fibers. That is, pores can be formed on PLGA fibers. For PVA, it is difficult to form breath figures since the solvent of PVA is water, thus pores are hardly formed on PVA fibers. The distinctions in beads formation of these fibers may mainly attribute to the different surface tension. The throughput of beads is positive correlation with the surface tension of homogeneous solution [19]. Therefore, PVA is easier to form beads since the surface tension of water is higher than that of methylene dichloride.

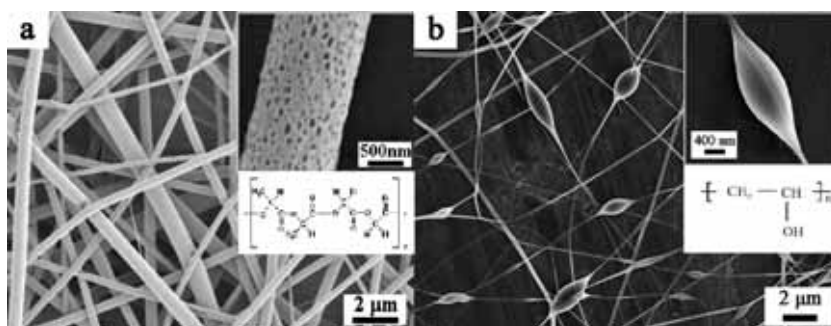


Fig. 1. SEM micrographs of PLGA EFMs (a) and PVA EFMs (b). The average diameters of the PLGA and PVA fibers are approximately 600 nm and 115 nm, respectively.

3.2. Sorption kinetics

Fig. 2. shows the sorption kinetics of PFOS on EFMs. the sorption equilibrium was almost achieved within the first 10 min of the reaction, and then became more gradual until the equilibrium was reached in 120 min. The sorption amount of EFMs for PFOS at 10 min were 30.98 and 30.57 $\mu\text{g}\cdot\text{g}^{-1}$, respectively. PFOM and PSOM were applied to describe the sorption kinetics data to further understand the sorption kinetics of PFOS on the EFMs. The fitting results indicate that the PFOM fits the experimental data better than the PSOM according to the higher correlation coefficient ($r^2 > 0.99$). It demonstrated that physical reactions play a key role in adsorption process. As an applicable rate constant, the parameter k_1 can directly describe adsorption kinetic process. The k_1 values of PFOS on PVA and PLGA EFMs were 0.490 and 0.307 h^{-1} , respectively. This result may be due to the hydrogen bonding interactions between sulfo group on PFOS and -OH group on PVA EFMs. Thus, hydrogen bonding interactions and Van der Waals force exist in the sorption processes of PFOS on PVA EFMs. However, PLGA EFMs contain no -OH group, so there is no hydrogen bonding interaction that exist in the sorption processes of PFOS on PLGA EFMs.

Compared with the q_t between PVA EFMs and PLGA EFMs, the differences could be observed after

the first 10 min. This phenomenon may result from the difference of pores on EFMs. PLGA EFMs contain plenty of pores, which provide enough space for the sorption of PFOS. This result shows that the process of PFOS adsorbed by PLGA EFMs contains two steps: (1) PFOS molecules diffuse from the bulk solution to the external surfaces of the PLGA EFMs, and adsorb on the surface, which is usually assumed to be a fast step; (2) PFOS molecules diffuse into the PLGA fibers through pores that is treated as a relative slow step. However, there are only surface adsorptions for PVA EFMs due to the fact that no pore was detected.

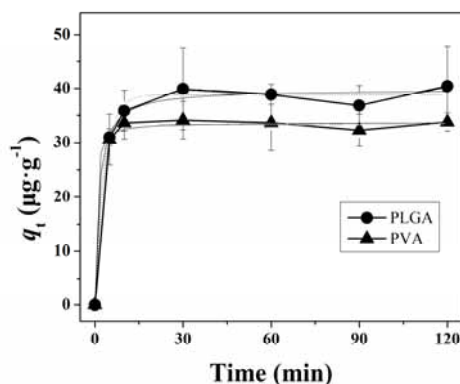


Fig. 2. Sorption kinetics of PCP on EFMs fitted by pseudo-first-order model (...) and pseudo-second-order model (—).

3.3. Sorption isotherms

The sorption isotherms for PFOS on EFMs are shown in Table 2. The results showed that sorption isotherms could be well fitted by both of them, supported by the high r^2 values ($r^2 > 0.97$). According to the results of Freundlich fitting (n^{-1}), the isotherms are nonlinear. It further demonstrates that hydrogen bonding interactions and Van der Waals force plays important roles in the sorption. According to the parameter Q_0 , the sorption capacity is 77.29 and 337.77 $\mu\text{g}\cdot\text{g}^{-1}$ for PVA and PLGA EFMs, respectively. This huge difference may also result from the difference of pores on EFMs. Furthermore, it demonstrated that pore-filling was the main mechanism for the sorption of PFOS on EFMs.

Table 2. The result of sorption isotherm of PFOS on EFMs fitted by Freundlich model and Langmuir model.

EFMs	n^{-1}	FM		$K_L[\mu\text{g/L}]$	LM	
		$K_f [(\mu\text{g/g})/(\mu\text{g/L})^{1/n}]$	r^2		$Q_0 (\mu\text{g/g})$	r^2
PVA	0.506	1.86	0.972	325.56	77.29	0.986
PLGA	0.687	1.58	0.990	934.24	337.77	0.978

4. Conclusions

PLGA and PVA were used to prepare the EFMs by electrospinning, respectively. PLGA EFMs possessed the feature of porous and bead-free. PVA EFMs contain plenty of beads and no pore is detected. Sorption kinetics data of PFOS on two types of EFMs indicate that the equilibrium was reached in 120 min and can be well fitted by the pseudo-first-order model (PFOM). The isotherm results show that the sorption capacities of PFOS on PLGA and PVA EFMs are 77.29 and 337.77 $\mu\text{g}\cdot\text{g}^{-1}$, respectively. The main sorption mechanisms of PFOS on PLGA EFMs are pore-filling. Moreover, hydrogen bonding

interactions exist in the sorption processes of PFOS on PVA EFMs.

Acknowledgements

This study was financially supported by the National Basic Research Program of China (973 Program, 2010CB429003), the Fund for Creative Research Groups of the National Natural Science Foundation of China (Grant No. 51121003), and the Program of the Co-Construction with Beijing Municipal Commission of Education of China.

References

- [1] Zhao YG, Wong CKC, Wong MH. Environmental contamination, human exposure and body loadings of perfluorooctane sulfonate (PFOS), focusing on Asian countries. *Chemosphere* 2012;4:355-68.
- [2] Paul AG, Jones KC, Sweetman AJA. First global production, emission, and environmental inventory for perfluorooctane sulfonate. *Environ. Sci. Technol.* 2009;2:386-92.
- [3] Wan HT, Zhao YG, Wei X, Hui KY, Giesy JP, Wong CKC. PFOS-induced hepatic steatosis, the mechanistic actions on beta-oxidation and lipid transport. *Biochim. Biophys. Acta-Gen. Subj.* 2012;7: 1092-101.
- [4] Senevirathna STMLD, Tanaka S, Fujii S, Kunacheva C, Harada H, Ariyadasa BHAKT et al.. Adsorption of perfluorooctane sulfonate (n-PFOS) onto non ion-exchange polymers and granular activated carbon: Batch and column test. *Desalination* 2010;1-3:29-33
- [5] Thompson J, Eaglesham G, Reungoat J, Poussade Y, Bartkow M, Lawrence M et al.. Removal of PFOS, PFOA and other perfluoroalkyl acids at water reclamation plants in South East Queensland Australia. *Chemosphere* 2011;1: 9-17.
- [6] Vecitis CD, Park H, Cheng J, Mader BT, Hoffmann MR. Treatment technologies for aqueous perfluorooctanesulfonate (PFOS) and perfluorooctanoate (PFOA). *Front. Environ. Sci. Eng. China* 2009;2:129-51.
- [7] Cheng J, Vecitis CD, Park H, Mader BT, Hoffmann MR. Sonochemical degradation of perfluorooctane sulfonate (PFOS) and perfluorooctanoate (PFOA) in groundwater: kinetic effects of matrix inorganics. *Environ. Sci. Technol.* 2010;1:445-50.
- [8] Li XN, Chen S, Quan X, Zhang YB. Enhanced adsorption of PFOA and PFOS on multiwalled carbon nanotubes under electrochemical assistance. *Environ. Sci. Technol.* 2011;19:8498-505.
- [9] Wang F, Shih KM. Adsorption of perfluorooctanesulfonate (PFOS) and perfluorooctanoate (PFOA) on alumina: Influence of solution pH and cations. *Water Res.* 2011;9:2925-30.
- [10] Wang F, Liu CS, Shih K. Adsorption behavior of perfluorooctanesulfonate (PFOS) and perfluorooctanoate (PFOA) on boehmite. *Chemosphere* 2012;8:1009-14.
- [11] Dai YR, Niu JF, Yin LF, Xu JJ, Xi YH. Sorption of polycyclic aromatic hydrocarbons on electrospun nanofibrous membranes: Sorption kinetics and mechanism. *J. Hazard. Mater.* 2011;3:1409-17.
- [12] Bhattarai SR, Bhattarai N, Yi HK, Hwang PH, Cha DI, Kim HY. Novel biodegradable electrospun membrane: scaffold for tissue engineering. *Biomaterials* 2004;25:2595-602.
- [13] Greiner A, Wendorff JH. Electrospinning: A fascinating method for the preparation of ultrathin fibres. *Angew. Chem. Int. Ed.* 2007;46:5670-703.
- [14] Kampalanonwat P, Supaphol P. Preparation and Adsorption Behavior of Aminated Electrospun Polyacrylonitrile Nanofiber Mats for Heavy Metal Ion Removal. *ACS Appl. Mater. Interfaces* 2010;12:3619-27.
- [15] Dai YR, Yin LF, Niu JF. Laccase-Carrying electrospun fibrous membranes for adsorption and degradation of PAHs in Shaoal Soils. *Environ. Sci. Technol.* 2011;24:10611-8.
- [16] Wu J, Wang N, Wang L, Dong H, Zhao Y, Jiang L. Electrospun porous structure fibrous film with high oil adsorption capacity. *ACS Appl. Mater. Interfaces* 2012;6:3207-12.
- [17] Megelski S, Stephens JS, Chase DB, Rabolt JF. Micro- and nanostructured surface morphology on electrospun polymer fibers. *Macromolecules* 2002;35:8456-66.
- [18] Casper CL, Stephens JS, Tassi NG, Chase DB, Rabolt JF. Controlling surface morphology of electrospun polystyrene fibers: Effect of humidity and molecular weight in the electrospinning process. *Macromolecules* 2004;2:573-8.
- [19] Lee KH, Kim HY, Bang HJ, Jung YH, Lee SG. The change of bead morphology formed on electrospun polystyrene fibers. *Polymer* 2003;14:4029-34.